Subalpine peatland development since the Last Glacial Maximum in subtropical China: Predominantly controlled by monsoonal climate and local topography

Cong Chen, Kangyou Huang, Dehao Xie, Meiling Man, Yongjie Tang, Yuanfu Yue, Xiao Zhang, Zhuo Zheng, Rachid Cheddadi

Subalpine peatland development since the Last Glacial Maximum in subtropical China: Predominantly controlled by monsoonal climate and local topography

Cong Chen[a], Kangyou Huang[a,b*], Dehao Xie[a,c], Meiling Man[d], Mengyuan Wang[b,e], Yongjie Tang[a], Yuanfu Yue[f], Xiao Zhang[a], Zhuo Zheng[a,b], Rachid Cheddadi[g]

[a] Guangdong Key Laboratory of Geodynamics and Geohazards, School of Earth Sciences and Engineering, Sun Yat-sen University, Zhuhai 519082, China;

[b] Southern Marine Science and Engineering Guangdong Laboratory (Zhuhai), Zhuhai 519082, China;

[c] Guangzhou Marine Geological Survey, Guangzhou 510760, China;

[d] Department of Physical and Environmental Sciences, University of Toronto Scarborough, Toronto, Canada;

[e] School of Marine Sciences, Sun Yat-Sen University, Zhuhai 519082, China;

[f] School of Marine Sciences, Guangxi University, Nanning 530004, China;

[g] Institute of Evolutionary Sciences of Montpellier, University of Montpellier, CNRS, Montpellier 34095, France.

*Corresponding authors: K.Y.H. (hkangy@mail.sysu.edu.cn).

Abstract

Peatlands have a great interaction with global carbon cycle and climate changes. A comprehensive understanding of carbon accumulation and development of peatlands is extremely important to help address future climate challenges. We here combine three total organic carbon content with seven published records from subalpine peatlands in monsoonal region of subtropical China, aiming to reveal the general pattern of carbon accumulation and development of peatlands since the Last Glacial Maximum (LGM) in this region. The synthesis show that carbon accumulation significantly increased at approximately 16 cal. ka BP, synchronous with a peak of peatland initiation in this region. Since then, these records clearly display two distinct patterns: Pattern one showed three intervals of high carbon accumulation at ca. 16–12 cal. ka BP, 9.5–7.5 cal. ka BP and 6–4 (or 4–1) cal. ka BP respectively, whereas pattern two reached the maximum in the early Holocene and kept stably high during the Holocene. Through comparing with pollen indicator and climate reconstruction, we demonstrated that hydrology linked to monsoonal climates (especially precipitation) was the dominant factor controlling carbon accumulation and development of subalpine peatlands since the LGM in subtropical China. However, two dynamic patterns occurred under the same climatic conditions were attributed to the significant modulation of local topography, i.e., intermontane basin (pattern one) or montane settings (pattern two). The hydrology and carbon accumulation of peatlands is a function of the changes in monsoonal climate and local site-specific topography. These findings provide a comprehensive understanding of past long-

term carbon accumulation and development of peatlands under monsoonal climate.

Keywords: carbon accumulation; peatland development; monsoonal climate; local topography; subtropical China; the Last Glacial Maximum

1. Introduction

Peatlands exert enormous influences on global carbon cycle and climate changes, owing to their high carbon accumulation rate, great greenhouse gas emissions (e.g., CH_4) and climate sensitivity (Ribeiro et al., 2021). Peatlands have accumulated one third of global terrestrial soil carbon since the Last Glacial Maximum (LGM, approximately 21,000 years ago) (Yu et al., 2010), a period of extreme climate and atmospheric CO_2 concentration variability (Shakun and Carlson, 2010) and an important time window for accessing past environmental fluctuations (Liu et al., 2022). Among them, northern (boreal and subarctic) and tropical peatlands have served as the major terrestrial carbon pools (Müller and Joos, 2020). Abrupt increases in global atmospheric CH_4 concentration that were coupled with rapid climate changes since the LGM, was also linked to northern and tropical peatlands (MacDonald et al., 2006). Considering the major role in moderating global climate, the understanding of past peatland development and related controlling factors is extremely important to help address future climate challenges. Studies suggest that the development of northern peatland on millennial to orbital timescales was mainly controlled by thermal condition and continental ice-sheet extents (Yu et al., 2010; Treat et al., 2019); whereas that of tropical peatland was predominately

driven by sea level changes and regional climate changes (Dommain et al., 2011; Treat et al., 2019).

Although the area is relatively small compared to the northern and tropical peatlands (Müller and Joos, 2020), subalpine peatlands in monsoonal region of subtropical China seem to be unique at these latitudes in the North Hemisphere (Yu et al., 2010) due to monsoonal climate. In subtropical China, peatlands commonly develop in mountains and are usually the water sources of rivers. Some peatlands (e.g., the Caohai and Dajiuhu peatlands) are also important habitats for endangered species and stop-over sites for migratory birds. Therefore, subalpine peatlands in subtropical China are of great significance in water resource management and biodiversity conservation (Huang et al., 2017; Zhang et al., 2021). Furthermore, peatlands in subtropical China are also an important source of greenhouse gases. For instance, they might have contributed to high atmospheric CH_4 concentrations during past warm intervals such as the Marine Isotope Stage 3 (MIS 3) and the Bølling-Allerød (B/A) period (Zhao et al., 2014; Xu et al., 2016). In addition, their sediments are valuable archives for paleoenvironment reconstructions (e.g., Zhong et al., 2010; Yue et al., 2012; Liu et al., 2020), for example, total organic carbon (TOC) contents as a proxy for the East Asia summer monsoon (EASM) intensity (e.g., Ma et al., 2009; Zhang et al., 2018).

Peatlands in subtropical China are proposed to be strongly influenced by the hydrology linked to monsoonal climate changes (Zhao et al., 2014; Zhang et al., 2016; Yu et al., 2020). Local factors such as topography and elevation that vary

significantly in subtropical China could also affect the development of subalpine peatlands (Zhao et al., 2014; Zhang et al., 2016). However, our knowledge of long-term (i.e., covering the last glacial-interglacial cycle) development of peatlands across a broad range of this subtropical region is still limited. Previous studies mostly focus on specific sites such as the Dajiuhu (Ma et al., 2009; He et al., 2015; Zhang et al., 2016), Dahu (Zhou et al., 2004; Wei et al., 2018; Yu et al., 2020) and Tengchong peatlands (Xu et al., 2016; Cui et al., 2023), which is insufficient to provide a fundamental and comprehensive understanding of carbon accumulation and development of peatlands in this region. Furthermore, ongoing global warming is likely to produce more frequent and severe climate changes in monsoonal region (IPCC, 2021), which may cause irreversible damages to the vulnerable mountain peatlands and ecosystems. Hence, subtropical China is an ideal region to decipher the controls of regional climate changes and/or local factors on past long-term carbon accumulation and development of peatland, helping the conversation of subalpine peatlands in this monsoonal region under projected climate changes.

In this study, we present three ca. 21,000-year TOC records obtained from the Caohainantun, Gutian and Huyangta peatlands, respectively. Then, through combining with seven published TOC records, we aim to reveal the general carbon accumulation pattern and development of subalpine peatlands in subtropical China during the last glacial-interglacial cycle (i.e., from the LGM to the Holocene). These records represent most geographic part of the study region and clearly display two distinct patterns. We further discuss the influences of monsoonal climate and local

topography on these two patterns, through comparing with regional climate reconstruction, pollen data of the same cores and local geomorphological settings.

2. Materials and Methods

2.1. Regional Settings

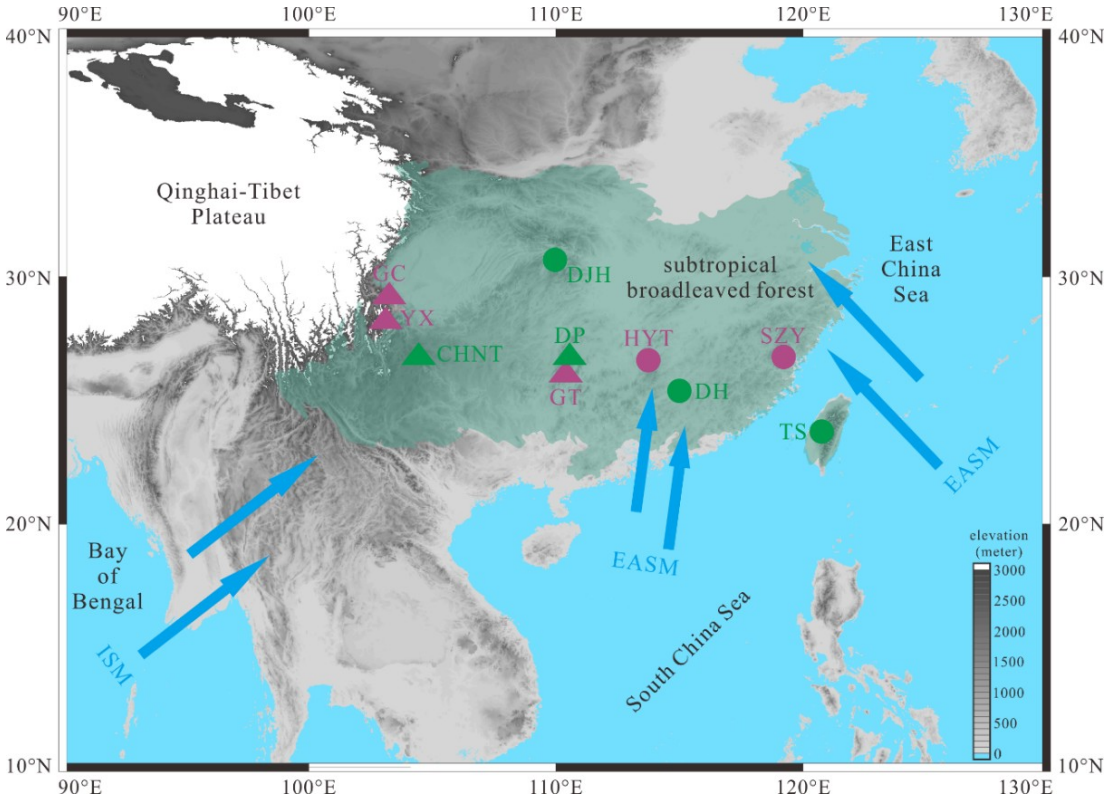

Fig. 1. Geographic map of the subtropical China (light green shade area). Details of peatlands in this study are listed in Table 1. Green triangles and dots - peatlands of pattern one; Purple triangles and dots - peatlands of pattern two. EASM - East Asian summer monsoon; ISM - Indian summer monsoon.

The present-day climate of subtropical China is dominantly influenced by the Asian monsoon. The precipitation is concentrated mostly from March to September, which is dominantly controlled by the EASM in the east part and the Indian summer monsoon (ISM) in the west part (Fig. 1). Regional vegetation is dominated by

subtropical broadleaved forests (Wu, 1980). However, vertical vegetation belts are common in mountain ranges of this region due to the varied topography and elevations (Zhang et al., 2020). The ten peatlands discussed in this study cover the region between ca. 23°N and 32°N and 102°E and 121°E (Table 1), west to the southeast margin of the Tibetan Plateau and east to the northwestern Pacific Ocean (Fig. 1). Their altitudes generally vary between ca. 250 m and 2200 m. Their mean annual temperature and precipitation range from 11 and 19 ℃ and 850 and 2000 mm, respectively. Furthermore, these peatlands locate at representative units of the study region: the Caohainantun, Yuexi and Ganchi peatlands are in the typical ISM region; the Huyangta, Dahu and Dajiuhu peatlands are in the typical EASM region; the Gutian and Daping peatlands are in a transitional zone between these two monsoon subsystems, but are still dominantly influenced by the ISM; the Shuizhuyang and Toushe peatlands are close to the Pacific Ocean (Fig. 1).

Table 1. Details of the ten peatlands in subtropical China discussed in this study.

No.	Peatland	Location	Elevation (m)	Age range (cal. ka BP)	Dating point	Geomorphological setting	Reference*
1	Ganchi (GC)	29.39°N, 103.03°E	1805	0–26.2	14	montane peatland	1
2	Yuexi (YX)	28.78°N, 102.95°E	1950	0–15.4	20	montane peatland	2
3	Caohainantun (CHNT)	26.81°N, 104.34°E	2165	0–21.0	9	intermontane basin	3
4	Gutian (GT)	26.09°N, 110.37°E	1677	0–21.1	10	montane peatland	3
5	Daping (DP)	24.76°N, 115.04°E	246	0–15.4	12	intermontane basin	4
6	Dajiuhu (DJH)	31.49°N, 110.00°E	1760	0–16.0	10	intermontane basin	5
7	Huyangta	26.46°N,	1486	0–21.8	5	montane peatland	3

	(HYT)	114.00°E					
8	Dahu (DH)	24.75°N, 115.03°E	260	0–18.0	10	intermontane basin	6
9	Shuizhuyang (SZY)	26.77°N, 119.03°E	1007	0–30.0	8	montane peatland	7
10	Toushe (TS)	23.82°N, 120.88°E	650	0–30.0	24	intermontane basin	8

*References: 1. Huang et al., 2022; 2. Peng et al., 2021; 3. This study; 4. Zhong et al., 2017; 5. Ma et al., 2009; 6. Zhou et al., 2004; 7. Wang et al., 2017; 8. Li et al., 2013.

2.2. Cores and Lithology

A continuous 405 cm-long sediment core (CHNT03) was collected from the Nantun peatland of the intermontane Caohai Basin, southwestern China in August 2013 (Table 1). The lithology is mainly gray-black clay and peat containing plant debris (50–380 cm) with cultivation disturbance at the top (0–50 cm), but turns into a thin sand-gravels layer at the base (380–405 cm) (Fig. 2a). Core GT (194 cm-long) was retrieved from a montane peatland (Gutian) in the west Nanling Ranges, southern China in June 2010 (Table 1). The lithology shows a thin sand layer interbedded with gravel at the base, gray silty clay at 140–190 cm, peat with abundant plant debris at 22–140 cm, and brown root-rich gyttja at the top (0–22 cm) (Fig. 2b). Core HYT is 265 cm-long and was collected from a montane peatland (Huyangta) in the Luoxiao Ranges, southern China in August 2017 (Table 1). This study focuses on the top 150 cm of core HYT, representing the time interval from ca. 21,000 cal a BP to present. The upper part of core HYT (0–95 cm) is mainly composed of peat sediments and dark gray clay, and the lower part turns into gray clay with fine sands (Fig. 2c). We collected these peat cores using a 50 cm-long Russian-type peat corer.

In the other hand, the Dajiuhu, Toushe, Daping and the Dahu peatlands develops in a relatively closed intermontane basin in the west Shennongjia Mountains (Ma et al., 2009), central Taiwan Island (Li et al., 2013), west (Zhong et al., 2017) and east Nanling Mountains (Yu et al., 2020), respectively. The Shuizhuyang, Ganchi and Yuexi peatlands are montane peatlands formed in the southeast Jiufeng Mountains (Yue et al., 2012), Dawa Mountain (Huang et al., 2022), and northeast Hengduan Mountains (Peng et al., 2021), respectively. All ten peatlands are without large inflow rivers and mostly fed by direct precipitation and runoff from the surrounding catchments.

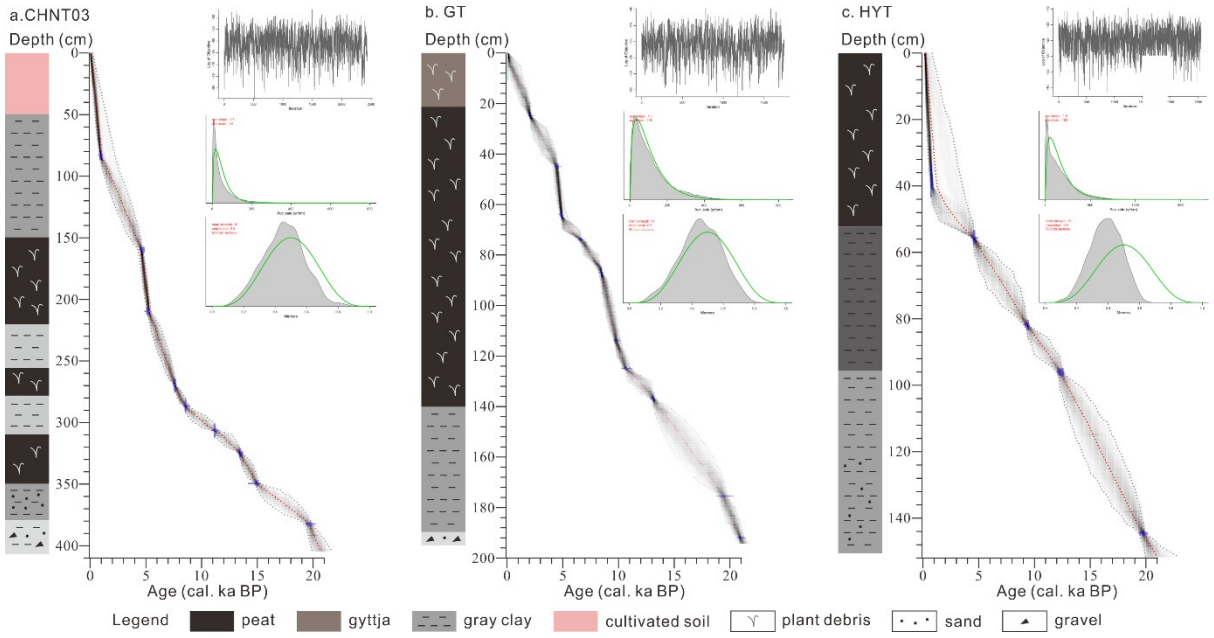

Fig. 2. Lithology and age-depth models of cores CHNT03, GT and HYT.

2.3. Radiocarbon Dating

The chronologies of three peat cores in this study are based on the accelerator mass spectrometry radiocarbon (AMS ^{14}C) dates of plant debris, bulk organic matter or pollen concentrates, pretreated using the standard acid-base-acid (ABA) method.

In total, 9, 10 and 5 AMS ^{14}C dates were obtained for cores CHNT03 (Zhang et al., 2023), GT (Zheng et al., 2023) and HYT, respectively. Conventional ages were calibrated to calendar years (i.e., cal. yr BP) using the IntCal20 calibration dataset (Reimer et al., 2020). Then, the age-depth models of these cores were established using the Bayesian approach implemented in the Bacon 2.2 package (Blaauw and Christen, 2011) for R program.

2.4. Proxy Measurements

In this study, the proxy of total organic carbon (TOC) content is used to indicate carbon accumulation in sediments and peatland development. The samples were firstly ground to < 200 mesh size and homogenized, followed in sequence by treated using 5% HCl to remove carbonate, adjusted to pH 7.0 with deionized water and then freeze-dried. TOC and total nitrogen (TN) contents were measured on a Vario EL cube Element Analyzer (standard deviations < 0.1%). Sampling resolutions are ca. 2 cm, 4 cm and 2 cm for cores CHNT03, GT and HYT, respectively. To validate the accuracy of TOC results, we also measured the proxy of loss in ignition (LOI) for samples of core CHNT03, following the procedures suggested by Heiri et al. (2001). Briefly, after overnight oven-drying of ca. 1.5 g sample at 105 ℃, organic matter was combusted at a temperature of 550 ℃ for 4 hours in a muffle. Loss in ignition at 550 ℃ (LOI_{550}) was then calculated using the following equation: $LOI_{550} = ((weight_{105} – weight_{505})/weight_{105}) *100$. All proxy measurements above were finished in the Instrumental Analysis and Research Center of Sun Yat-sen University.

We also conducted pollen analysis on samples of cores CHNT03 and GT using a

standard method (Moore et al., 1991) with minor amendment, i.e., treated by 10% HCl and 10% KOH to remove carbonates and turbid organic matter, respectively, followed by density separation using iodine dense liquid (2.0 g/m^3) (Huang et al., 2014). A tracer tablet containing 27,637 *Lycopodium* spores was added to each sample to allow pollen concentration to be calculated. Pollen percentages were calculated based on the sum of terrestrial pollen, excluding aquatic pollen (e.g., Cyperaceae) and spores. Based on the pollen data of core CHNT03, paleoclimate variables (i.e., mean annual temperature and precipitation) were quantitatively reconstructed using a transfer function method (the Locally Weighted-Weighted Average Partial Least Squares, LW-WAPLS) (Birks et al., 2012) based on the updated Eastern Asia Pollen Dataset (EAPD) (Zheng et al., 2014). Results of pollen analysis and climate reconstructions have been presented in our previous studies (Zhang et al., 2023; Zheng et al., 2023).

3. Results

3.1. Dating results

The AMS ^{14}C dates of three peat cores presented in this study were all in stratigraphic order and increased with depth (Table 2), respectively. Age-depth models show that all of these cores cover the last ca. 21,000 cal a BP (Fig. 2), ranging from the LGM to the Holocene (Clark et al., 2009). Mean sedimentation rates are significantly different between these cores, i.e., ca. 19.4 cm/kyr, 9.3 cm/kyr and 7.1 cm/kyr for cores CHNT03, GT and HYT, respectively. Thus, we propose that the

sampling resolutions (i.e., 103 yr, 430 yr and 282 yr, respectively) are efficient to capture millennial- to orbital-scale variations in TOC contents and consequently carbon accumulation of these records. According to the lithology and dating results, no obvious sedimentary hiatus was found. In addition, the published TOC records from the Ganchi, Dahu, Shuizhuyang and Toushe peatlands extend to the LGM, while the basal ages of records from the Yuexi, Daping, Dahu and Dajiuhu peatlands are approximately 16 cal. ka BP (Table 1).

Table 2. Accelerator mass spectrometry radiocarbon (AMS ^{14}C) dating results of cores CHNT03 (Zhang et al., 2023)**, GT** (Zheng et al., 2023) **and HYT in this study.**

Core	Sample	Depth (cm)	Material	^{14}C age ± error (BP)	2σ (cal. BP)
CHNT03	NT-83*	83	plant debris	950±30	788–922
	NT-160#	160	bulk organics	4131±32	4529–4821
	NT-210#	210	wood fragment	4520±24	5051–5307
	NT-270#	270	bulk organics	6772±30	7578–7670
	NT-287*	287	bulk organics	7820±30	8521–8696
	NT-307*	307	bulk organics	9850±40	11196–11390
	NT-325#	325	bulk organics	11709±47	13462–13742
	NT-350#	350	bulk organics	12638±43	14924–15220
	NT-383*	383	bulk organics	16490±70	19613–20122
GT	GT-25*	25	pollen concentrates	2030±30	1882–2096
	GT-45†	45	pollen concentrates	3970±40	4292–4526
	GT-64§	64	bulk organics	4233±28	4651–4856
	GT-74†	74	pollen concentrates	5740±70	6353–6729
	GT-87*	87	bulk organics	7650±40	8381–8537
	GT-114§	114	bulk organics	8738±43	9552–9892
	GT-125†	125	pollen concentrates	9390±70	10382–11063
	GT-137*	137	bulk organics	11250±60	13086–13296
	GT-175†	175.5	pollen concentrates	16170±140	19147–19878
	GT-192§	192	bulk organics	17395±66	20821–21250
HYT	HYT-38*	38	bulk organics	530±30	511–625
	HYT-55*	55	bulk organics	3990±30	4409–4526
	HYT-81*	81	bulk organics	8330±30	9151–9458
	HYT-95*	95	bulk organics	10450±30	12105–12611
	HYT-143*	143	bulk organics	16500±50	19621–20127

Dating labs: *Beta Analytic Inc.; #Institute of Earth Environment, Chinese Academy of Sciences (CAS); †Poznan Radiocarbon Laboratory; §Guangzhou Institute of Geochemistry, CAS.

3.2. TOC, TN and LOI results

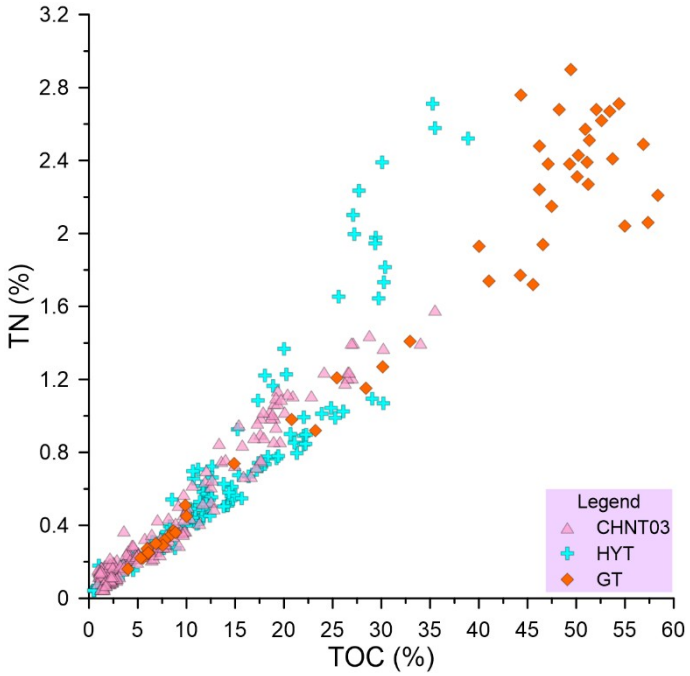

Fig. 3. The TOC values plotted against TN values of core CHNT03, core GT and core HYT. Generally, TOC of these cores are correlated with the corresponding TN towards the origin.

TOC values of cores CHNT03 and HYT vary between 0% and 40%, and values of core GT could increase to ca. 60% (Fig. 3). Generally, variations in TOC content are consistent with the lithology, i.e., high values (> 20%) in peat with abundant plant debris, relatively low values (5–10%) in gray silty clay and lowest values (< 5%) in basal sand layers. TOC contents of three cores are correlated with the corresponding TN contents towards the origin (Fig. 3), indicating that TOC results are not significantly influenced by inorganic carbon and mostly resulted from organic matter deposit in sediments (Mampuku et al., 2008). In the other hand, we here use 48% carbon in sediment LOI for estimating the carbon content as suggested by

previous study in this region (Wei et al., 2018). Variations in estimated carbon content based on LOI results show good agreement with the TOC record in core CHNT03 (Fig. 4d), validating the accuracy of the proxy measurements. All available data taken together, we suggest that TOC variability in this study is related to the preservation of autochthonous and allochthonous organic matter in the sediments and thus could indicate carbon accumulation and development of peatlands.

4. Discussion

4.1. Two dynamic patterns of carbon accumulation since the LGM

TOC values at these peatlands excepting the Toushe maintained stable and low (generally < 5%) until ca. 16 cal. ka BP (Fig. 4), indicating low carbon accumulation and scare peatland development during the LGM in subtropical mountains of China. Since then, carbon accumulation dynamic within these ten peatlands clearly displayed two distinct patterns. Pattern one, including the Caohainantun, Daping, Dajiuhu, Dahu and Toushe peatlands, experienced an abrupt increase in TOC values at approximately 16 cal. ka BP after the Heinrich Event 1 (HE1). Since then, these five records show three intervals of high carbon contents at ca. 16–12 cal. ka BP (HC-I), 9.5–7.5 cal. ka BP (HC-II) and 6–4 cal. ka (HC-IIIa) BP respectively (Fig. 4b-f), except the latest interval of the Dajiuhu and Daping records at 4–1 cal. ka BP (HC-IIIb) (Fig. 4e and 4f). TOC values were generally higher than 20% during these intervals, but duration and values of the mid-interval (HC-II) were relatively short and small relative to the other two intervals (HC-I and HC-III). By contract, TOC values decreased below 10% during the periods between these intervals (HC-I, II, III).

Pattern two, including the Yuexi, Ganchi, Gutian, Huyangta and Shuizhuyang peatlands, mildly increased from approximately 16 cal. ka BP to 13.5 cal. ka BP. Then they accelerated toward the early Holocene (approximately 10 cal. ka BP). During the Holocene, TOC values generally maintained high with some centennial-scale fluctuations in peatlands of pattern two (Fig. 4g-k).

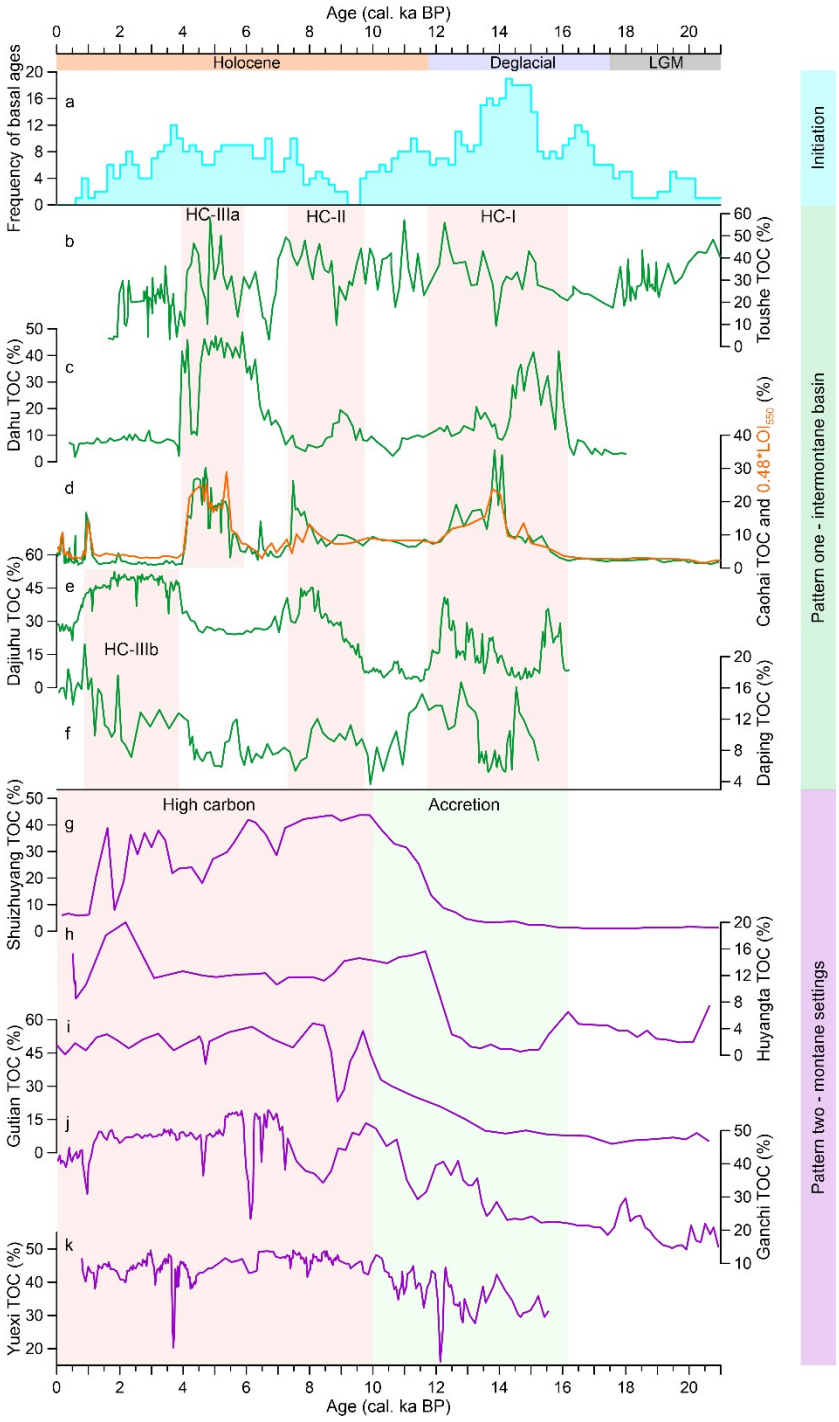

Fig. 4. Two dynamic patterns of carbon accumulation and development of subalpine peatlands since the Last Glacial Maximum (LGM) in subtropical China. (a) Frequency of basal peat ages in 200-year bins in subtropical China (Zhao et al., 2014); **(b-k)** Total organic carbon (TOC) records showing two distinct dynamic patterns of carbon accumulation and development of subalpine peatlands since the LGM in subtropical China. Details of peatlands in this study are listed in Table 1.

In general, TOC records from the study region covering relatively short periods or in poor resolution (e.g., He et al., 2015; Zhang et al., 2016; Huang et al., 2018; Dodson et al., 2021) are in consistence with the two patterns observed in this study. This broad-scale consistence points to that the two patterns of carbon accumulation and development of subalpine peatlands since the LGM were generally common (though not unique) in subtropical China. Moreover, the patterns have not significant relationship with the elevations of these peatlands or their geographic locations in the EASM or ISM subsystem. For example, the Caohainantun and Yuexi peatlands (Peng et al., 2021) locate at the same monsoon subregion (Wang and Ho, 2002) and have similar elevations (approximately 2000 m). However, their TOC records reveal significantly different history of carbon accumulation and peatland development since the LGM (Fig. 4d and 4k).

Interestingly, two high carbon intervals (HC-I and HC-III) of pattern one observed in this study are synchronous with high frequency of basal peat ages at approximately 16–13 cal. ka BP (i.e., the Bølling-Allerød period) and in the mid-late Holocene (Fig. 4a) (Zhao et al., 2014; Le et al., 2021), respectively. In particular, TOC values were larger than 30% (corresponding to > 60% organic matter in

sediments) in peatlands of pattern one (excepting the Daping) during the Bølling-Allerød warm period, which coincided with the maximum frequency of basal peat ages since the LGM in subtropical China (Zhao et al., 2014). Basal date indicates the time of peatland initiation; hence, an interval of high frequency of basal peat ages indicates a peak period of peatland initiation in a region (MacDonald et al., 2006). This correlation indicates a synchronous relationship between substantial peatland initiation and high carbon accumulation in subtropical China during the Bølling-Allerød warm period and the mid-late Holocene.

Although they are also influenced by the Asian monsoon, the dynamics of peatland initiation and carbon accumulation since the LGM in the Qinghai-Tibet Plateau and Northeast China, two major regions of peatland distribution in East Asia (Liu et al., 2020; Zhang et al., 2023), were quite different from those of subtropical peatlands observed in this study. In the Qinghai-Tibet Plateau, the peaks of peatland initiation and carbon accumulation were decoupled, i.e., at approximately 11.5–10 cal. ka BP and 9–7 cal. ka BP, respectively (Xu et al., 2013; Wang et al., 2014), in contract to the synchronous relationship in subtropical peatlands (Zhao et al., 2014; this study). In Northeast China, increase in carbon accumulation was coincided with the peatland expansion during the Holocene (particularly the mid-late Holocene) (Zhang et al., 2015; Zhang et al., 2023), significant later than the timing of the Bølling-Allerød warm period (ca. 16–13 cal. ka BP) in subtropical peatlands (Zhao et al., 2014; this study). These discrepancies indicate that the factors and mechanisms controlling peatland development in East Asia are very complicated and regionally

discrepant.

4.2. Dominant control of monsoonal climates on carbon accumulation

Two distinct patterns of carbon accumulation and development of subalpine peatlands since the LGM are observed in subtropical China (Fig. 4), regardless of their elevations and geographic locations in the EASM or ISM subsystem (Table 1). We here chose the Caohainantun and Gutian peatlands from the same monsoon (i.e., ISM) subsystem to reveal the mechanism and driving factors behind, avoiding the possible influence resulting from different monsoon subsystems. Their TOC records were compared with regional climate changes and local environments reconstructed from the same cores (Zhang et al., 2023; Zheng et al., 2023), which could avoid the disadvantage of age uncertainties resulting from record correlation between different cores.

Hydrology of peatlands is fundamental to their carbon dynamics (Holden, 2005), prominently shifting the oxic-anoxic boundary through water table fluctuations (Limpens et al., 2008). Therefore, we here first compared the TOC records to local hydrology variability since the LGM. In this study, the percentage of Cyperaceae pollen is used as an indicator of change in local hydrological environment. In humid monsoon region of East Asia, Cyperaceae are often of wetland habitats (Chen et al., 1987; Yue et al., 2012), which is unsuitable to grow in conditions of high water-level or arid soils. A similar trend in Cyperaceae pollen and *n*-alkanes proxy during the past 50 ka from a wetland in this region also demonstrates the close relationship between Cyperaceae and water-level (Tian et al., 2019). Therefore, the percentage

of Cyperaceae pollen could be used as an indicator of hydrological environment change in peatland.

In the Caohainantun and Gutian peatlands, the percentages of Cyperaceae pollen were closely correlated with the variations in TOC values (Figs. 5 and 6). Correlation coefficient (r) between TOC and Cyperaceae values based on the same samples were 0.65 ($n=90$, $p<0.01$) and 0.40 ($n=43$, $p<0.0.1$) in cores CHNT03 and GT (Fig. 5), respectively, before approximately 2 cal. ka BP when human-induced impacts on vegetation became significant (Cao et al., 2022; Zheng et al., 2023). Correlation coefficient could also increase to 0.60 ($n=34$, $p<0.01$) during the interval of 2–17 cal. ka BP in core GT. Specifically, the percentages of Cyperaceae pollen in core CHNT03 abruptly increased from 0% before 16 cal. ka BP to 28.6% during the Bølling-Allerød warm period, consistent with the abrupt changes in TOC values (Fig. 6d and 6e). In the Gutian peatland, relatively stable and high carbon contents corresponded to abundant Cyperaceae pollen during the Holocene (Fig. 6g and 6h). Strong correlation between TOC and Cyperaceae pollen demonstrates the primary influence of local hydrological environment on carbon accumulation and development (Limpens et al., 2008) of subalpine peatlands in subtropical China.

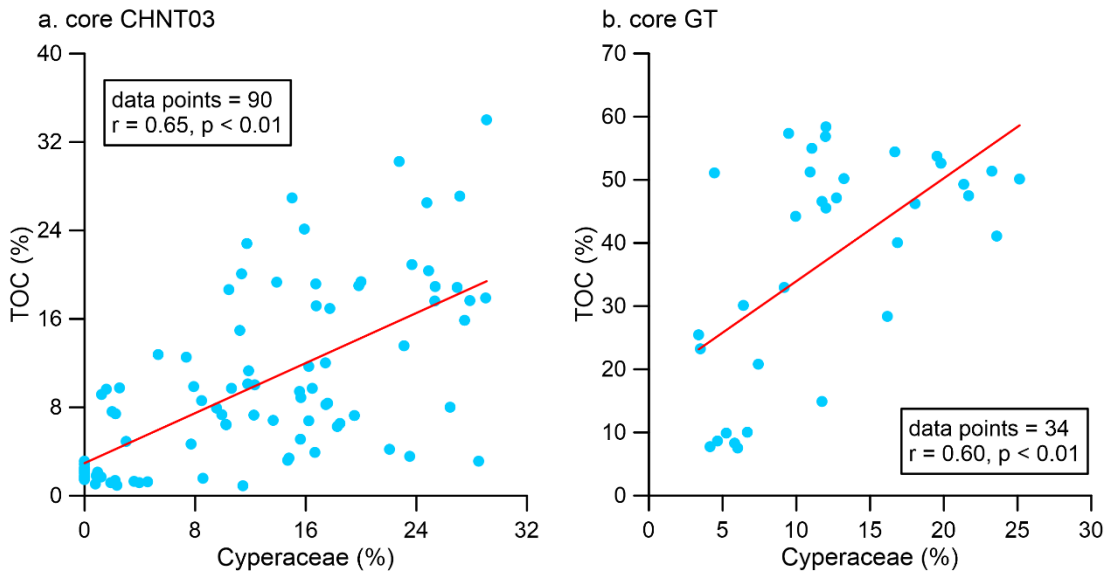

Fig. 5. Correlation between TOC and Cyperaceae pollen based on the same samples in the cores (a) CHNT03 (2–21 ka) and (b) GT (2–17 ka).

Then the TOC and pollen records were compared to regional climate changes since the LGM, given the high sensitivity of regional peatland hydrology to monsoonal climates (Wang et al., 2014; Zhao et al., 2014). Climate reconstruction (i.e., mean annual temperature and precipitation) from the Caohainantun peatland shows an agreement with pollen-based reconstruction from the Tengchongqinghai Lake (Zhang et al., 2023) and stalagmites $\delta^{18}O$ record from the CBoB caves close to the ISM moisture source (Liu et al., 2020). This agreement suggests that the reconstruction from the Caohainantun peatland (Zhang et al., 2023) could represent monsoonal climate changes since the LGM in the ISM region. As shown in Fig. 6, regional climate generally became warmer and wetter since the LGM (Fig. 6). Specifically, mean annual temperature (MAT) gradually increased since 18 cal. ka BP (Fig. 6a), slightly earlier than the increases in peatland initiation and carbon

accumulation (Fig. 4). However, mean annual precipitation (MAP) slightly decreased from 21 cal. ka BP to ca. 16 cal. ka BP, and significantly increased after the Heinrich Event 1 (Fig. 6b), which was synchronous with the abrupt increase in TOC and Cyperaceae values at 16 cal. ka BP in the same core (CHNT03) (Fig. 6d). Meanwhile, carbon accumulation in Gutian peatland also significantly increased (Fig. 6g). These relationships indicate that the initiation and carbon accumulation of peatland during the last deglacial in subtropical China were dominantly controlled by local hydrology linked to regional climate (especially monsoonal precipitation) changes, as suggested by previous studies (Zhao et al., 2014; He et al., 2015; Le et al., 2021).

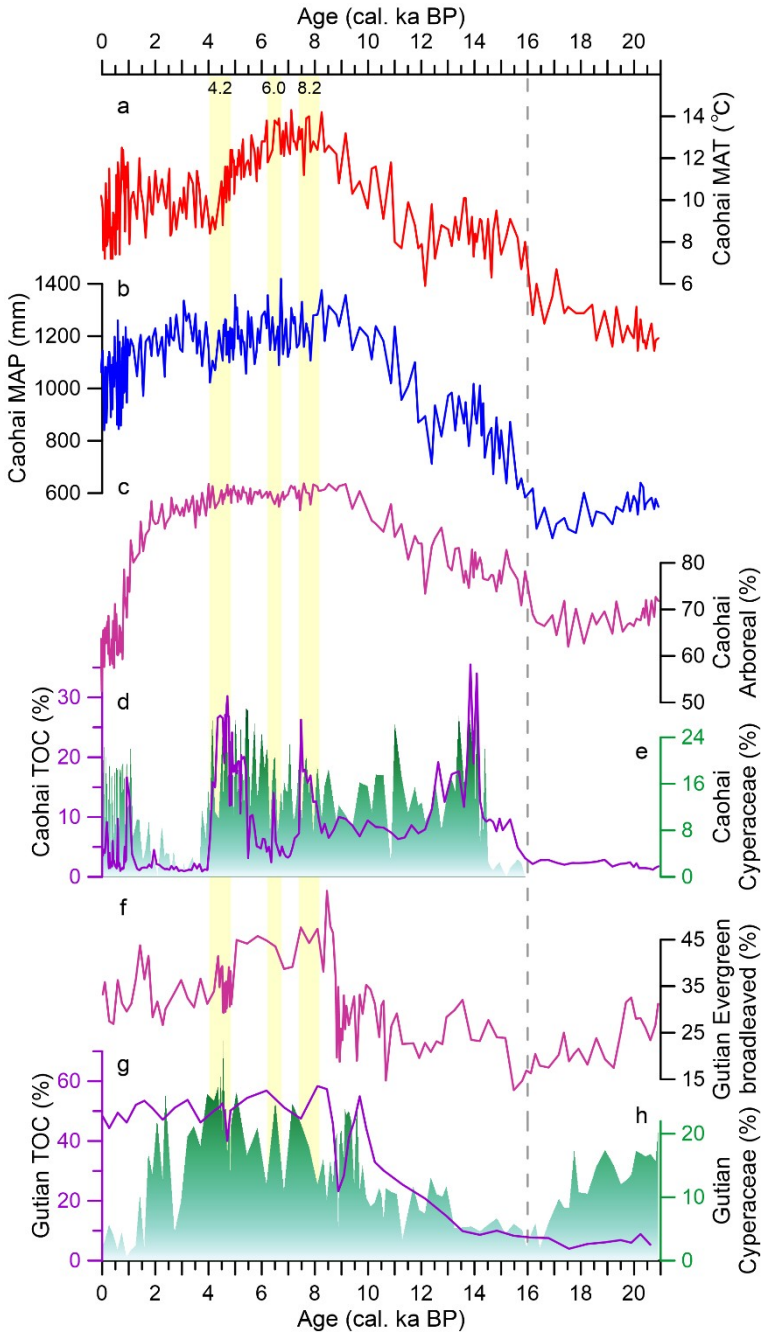

Fig. 6. Comparison between climate reconstruction, pollen data and total organic contents based on the same cores retrieved from the Caohainantun and Gutian peatlands.

Peatlands generally develop under the waterlogged conditions, and stably saturated water is necessary for the formation and maintenance of peatlands (Charman et al., 2009). Modern monitoring in the Dajiuhu peatland demonstrates

that approximately 30 cm of water table depth below the peatland surface is a critical level affecting the structure and function of peatland ecosystem and carbon sequestration (Liu et al., 2022). During the LGM, the precipitation and temperature were lower up to 50% and 7 ℃ in relative to the Holocene optimum (Zhang et al., 2023). Relatively cooler and/or drier conditions were not suitable for maintaining necessary water table, limiting carbon accumulation and thus peatland formation. Nevertheless, the improvement of monsoonal climate after the LGM facilitated the extensive initiations of peatland in subtropical region, as evidenced by the maximum frequency of basal peat ages since the LGM (Zhao et al., 2014). Meanwhile, favorable climate conditions also elevated vegetation coverage and net primary productivity in peatland and surrounding catchment. For example, the percentage of arboreal pollen in core CHNT03 significantly increased from 65% at 17 cal. ka BP to 80% at 15 cal. ka BP (Fig. 6c) (Zhang et al., 2023). Raising taxonomic richness and pollen concentration at the same time were also observed in the Shuizhuyang peatland (Yue et al., 2012). In the other hand, intensified monsoonal rainfall also enhanced the surface runoff and thus the input of allochthonous organic matter to peatland. In summary, favorable climate conditions (especially enhanced precipitation) after the LGM increased the net primary productivity in peatland and surrounding catchment and the input of allochthonous of organic matter, which both contributed to the formation and enhanced carbon accumulation in subtropical peatlands since approximately 16 cal. ka BP.

4.3. Significant modulations of local topography on carbon accumulation

Carbon accumulation and development of subalpine peatlands in subtropical China since ca. 16 cal. ka BP displayed two distinct patterns (Fig. 4b-k) under the same monsoonal climate conditions. Furthermore, TOC and Cyperaceae pollen in the Caohainantun peatland were negatively correlated with MAP variability during the Holocene, differing from the positive correlation during the last deglaciation. For example, intensified monsoonal precipitation was synchronous with the increases in TOC and Cyperaceae pollen during the Bølling-Allerød warm period (Fig. 6b and 6d). However, when ISM weaken and precipitation reduced during the 8.2 ka, 6.0 ka and 4.2 ka events (Wang et al., 2005; Lin et al., 2022; Chen et al., 2023), TOC and Cyperaceae pollen increased in the Caohainantun peatland (Fig. 6b and 6d). In the Gutian peatland, TOC and Cyperaceae pollen kept relatively stable during the mid-late Holocene, and did not follow the long-term decreasing trend of temperature and monsoonal precipitation since the mid-Holocene (Fig. 6b and 6g).

We attribute these to the modulation of local topography on the hydrology and thus carbon accumulation of peatlands in subtropical China. Generally, peatlands can form along two pathways: drying from an aquatic environment or wetting from a dryland (Charman, 2002). The peatlands of pattern one (e.g., the Caohainantun) developed in the closed intermontane basins with relatively large catchments (Fig. 7a). Therefore, when Asian summer monsoon intensified at ca. 16 cal. ka BP (Fig. 6b) (Zhang et al., 2023), surface runoff from the surrounding catchment fed by monsoonal precipitation flowed into the intermontane basin. Slight increases in monsoonal precipitation were enough to raise the water table of the basin due to

relatively large catchment, and thus strongly promoted peatland development and carbon accumulation (i.e., dryland-peatland transition) (Fig. 7b) as indicated by the sharp increase in TOC values (Fig. 6d). The initiation of wetland environment was also evidenced by the dramatic expansion of Cyperaceae vegetation (Fig. 6e). Subsequently, with the gradual intensification of monsoonal precipitation, water-level in peatland continuously increased because of lacking significant outflow river. Consequently, peatland was submerged and converted to a lake (i.e., peatland-lake transition) during the early Holocene (Fig. 7c). As a result, the sediment types changed from peat deposits with abundant plant debris to gray limnic clay sediments (Fig. 2a) with relatively low TOC values (generally 5-10%) (Fig. 6d) in the coring site. Meanwhile, the percentage of Cyperaceae pollen also declined (Fig. 6e), because high water-level was unsuitable to their growth.

Monsoonal precipitation recorded in core CHNT03 maintained relatively high during the Holocene, but showed a generally decreasing trend since the mid-Holocene (Fig. 6b). In addition, monsoonal precipitation experienced sharp decreases during the 8.2 ka, 6.0 ka and 4.2 ka cold events (Wang et al., 2005; Lin et al., 2022; Chen et al., 2023), synchronous with significant increases in TOC and Cyperaceae values in the same core (Fig. 6d and 6e). The basin is mainly fed by direct precipitation without major inflow. Therefore, the declines of precipitation resulted in the lowering of lake level and thus changed the lacustrine environment back into short-term peatland (i.e., lake-peatland transition) during the centennial-scale cold events. The limnic sediment might provide the suitable nutrients for the re-

colonization of peatland plants (Zhang et al., 2019). TOC values in core CHNT03 increased to large than 20% during the 8.2 ka and 4.2 ka cold events, similar to the values during the Bølling-Allerød warm period (Fig. 6d).

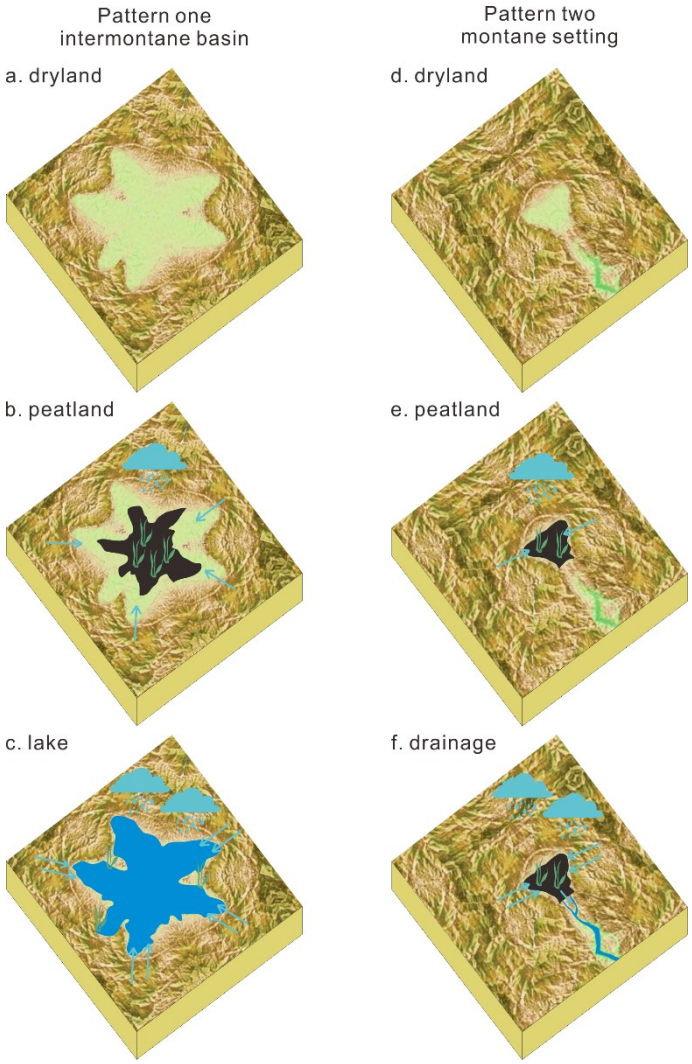

Fig. 7. Schematic of two development patterns for subalpine peatlands in subtropical China. (a-c) Pattern one: intermontane basin without obvious outflow. Peatland was submerged and converted to a lake when precipitation was high. **(d-f)**. Pattern two: montane setting. Excess water supply was not held by peatland but released as outflow to downslope parts in mountains.

Differently, peatlands of pattern two (e.g., the Gutian) are in montane settings with relatively small catchment (Fig. 7d). Since ca 16 cal. ka BP, water supply from

precipitation and surface runoff only increased slightly due to relatively small catchment, which could restrict the peatland development and carbon accumulation. Nevertheless, continuously enhanced water supply in association with gradual intensified monsoon precipitation elevated the water table in peatland, benefiting the carbon accumulation and thus peatland development in the early Holocene (i.e., dryland-peatland transition) (Fig. 7e). Their TOC records generally maintained relatively stable and high values during the Holocene soon afterwards (Fig. 4g-k). This was also attributed to the modulation of local topography. Peatlands of pattern two are semi-closed with outflow. Therefore, there is a critical threshold that these montane peatlands could kept water balance rather than turned into lake, despite monsoonal precipitation continuously increased. Instead, excess water supply from direct precipitation and runoff was not held by peatland but released as outflow to downslope parts in mountains (Fig. 7f). The relatively stable water depth might make the hydrology of peatlands less sensitive to monsoonal precipitation changes (Klein et al., 2013).

Interestingly, local topography could have contrary influences on carbon accumulation in peatlands of two patterns under the same monsoonal climate. For example, abrupt declines of monsoonal precipitation during the 8.2 ka and 4.2 ka events (Fig. 6b) resulted in increasing carbon contents in the Caohainantun peatland (pattern one) (Fig. 6d), but decreasing carbon contents in the Gutian peatland (pattern two) (Fig. 6g). These contrary influences of topography suggest that more attentions should be paid when the proxy of organic matter (e.g., TOC and LOI) is

used as the indicator of monsoon intensity/precipitation. It worth noting that although these two patterns are common in the study region, variations in TOC records within the same pattern were not tightly synchronous (Fig. 4b-k). Here, we suggest that the age discrepancies of the peatland development were also attributed to the local site-specific topography conditions such as basin/peatland sizes and depth, and/or partly age uncertainty. Similarly, variations in TOC records retrieved from different sites within a same basin may be also asynchronous (van Bellen, et al., 2011; Zhang et al., 2016). Two patterns observed in this study are representing general carbon accumulation dynamic and peatland development since the LGM in subtropical China, rather than the detailed process in a specific basin.

5. Conclusion

Ten TOC records are compiled to identify the general carbon accumulation and development of subalpine peatlands since the LGM in subtropical China. These records clearly display two distinct dynamic patterns. Local hydrology linked to regional monsoon climate (especially precipitation) was the dominant factor controlling regional peatland development since the LGM. However, this process was modulated significantly by local topography, i.e., intermontane basin (pattern one) or montane settings (pattern two). Local topography could have contrary influences on carbon accumulation in peatlands of two patterns under the same monsoon subsystem. Therefore, the hydrology and carbon accumulation of peatlands are a function of regional climate changes and local topography. The dynamics of peatland development in subtropical monsoonal region differed from

those in the Qinghai-Tibet Plateau and Northeast China, which could increase the complexity of the peatland management and the projection of carbon cycles and greenhouse gas emissions under global warming in China.

Declaration of Competing Interest

The authors declare that they have no known competing financial interests or personal relationships that could have appeared to influence the work reported in this paper.

Data availability

Data will be made available on request.

Acknowledgments

This work was supported by the National Key Research and Development Program of China (Grant number 2022YFF0801501), the National Natural Science Foundation of China (Grant number 42077414), the Project funded by China Postdoctoral Science Foundation (Grant number 2021M703659), and Innovation Group Project of Southern Marine Science and Engineering Guangdong Laboratory (Zhuhai) (Grant number 311022002). We would like to thank Aiyan Han, Kaixuan Liang, Xiaofei Gong, Jie Li and Huiwei Zheng for their help with fieldwork and laboratory measurements. We are also grateful to Prof. Yan Zhao from the Chinese Academy of Sciences for providing the data of basal peat ages in subtropical China.

References

Blaauw, M., Christen, J.A., 2011. Flexible paleoclimate age-depth models using an autoregressive gamma process. Bayesian Anal. 6, 457–474. https://doi.org/10.1214/ba/1339616472

Birks, H.J.B., Lotter, A.F., Juggins, S., Smol, J.P., 2012. Tracking evironmental change using lake sediments volume 5: Data handling and numerical techniques. Springer, Dordrecht.

Cao, X.Y., Tian, F., Herzschuh, U., Ni, J., Xu, Q.H., Li, W.J., Zhang, Y.R., Luo, M.Y., Chen, X.Y., 2022. Human activities have reduced plant diversity in eastern China over the last two millennia. Glob. Change Biol. 28, 4962–4976. https://doi.org/10.1111/gcb.16274.

Charman, D.J., 2002. Peatlands and Environmental Change. John Wiley and Sons, Chichester.

Charman, D.J., Barber, K.E., Blaauw, M., Langdon, P.G., Mauquoy, D., Daley, T.J., Hughes, P.D.M., Karofeld, E., 2009. Climate drivers for peatland palaeoclimate records. Quat. Sci. Rev. 28, 1811–1819. https://doi.org/10.1016/j.quascirev.2009.05.013

Chen, Y.D., 1987. A study on the cyeraceae plants in Qinghai Lake. Bull. Bot. Res. 7(2), 115–128

Clark, P.U., Dyke, A.S., Shakun, J.D., Carlson, A.E., Clark, J., Wohlfarth, B., Mitrovica, J.X., Hostetler, S.W., McCabe, A.M., 2009. The Last Glacial Maximum. Science 325, 710–714. https://doi.org/10.1126/science.1172873

Cui, K., Wang, Y.B., Liu, X.Q., Shen, J., Wang, Y., 2023. Holocene organic carbon burial in southwest China and potential response to climate variations. Catena 231, 107316. https://doi.org/10.1016/j.catena.2023.107316

Dodson, J., Shi, G., Lu, F.Y., Yan, H., 2021. A 40,000 year record of vegetation, environment and climate change from Chongqing, Central China. Palaeogeogr. Palaeoclimatol. Palaeoecol. 573, 110441. https://doi.org/10.1016/j.palaeo.2021.110441

Dommain, R., Couwenberg, J., Joosten, H., 2011. Development and carbon sequestration of tropical peat domes in south-east Asia: links to post-glacial sea-level changes and Holocene climate variability. Quat. Sci. Rev. 30, 999–1010. https://doi.org/10.1016/j.quascirev.2011.01.018

He, Y.X., Zhao, C. Zheng, Z., Liu, Z.H., Wang, N., Li, J., Cheddadi, R., 2015. Peatland evolution and associated environmental changes in central China over the past 40,000 years. Quat. Res. 84, 255–261. https://doi.org/10.1016/j.yqres.2015.06.004.

Heiri, O., Lotter, A.F., Lemcke, G., 2001. Loss on ignition as a method for estimating organic and carbonate content in sediments: reproducibility and comparability of results. J. Paleolimnol. 25, 101–110. https://doi.org/10.1023/A:1008119611481

Holden, J., 2005. Peatland hydrology and carbon release: why small-scale process matters. Phil. Trans. R. Soc. A 363, 2891–2913. https://doi.org/10.1098/rsta.2005.1671

Huang, K.Y., Zheng, Z., Liao, W.B., Cao, L.L., Zheng, Y.W., Zhang, H., Zhu, G.Q., Zhang, Z., Cheddadi, R., 2014. Reconstructing late Holocene vegetation and fire histories in monsoonal region of southeastern China. Palaeogeogr. Palaeoclimatol. Palaeoecol. 393, 102–110. https://doi.org/10.1016/j.palaeo.2013.11.005

Huang, K.Y., Xie, D.H., Chen, C., Tang, Y.J., Wan, Q.C., Zhang, X., 2023. An environmental crisis and its cultural impact in eastern China around 6000 years ago. Palaeogeogr. Palaeoclimatol. Palaeoecol. 624, 111652. https://doi.org/10.1016/j.palaeo.2023.111652

Huang, M., Deng, Y.K., Peng, H.J., Wen, Z.M., Shang, G.C., Guan, H.C., Ma, C.M., 2022. Hydroclimatic changes since the Last Glacial Maximum recorded in mountain peat deposit on the southwestern margin of the Sichuan Basin, China. Front. Ecol. Evol. 10, 1050429. https://doi.org/10.3389/fevo.2022.1050429

Huang, X.Y., Zhang, Z.Q., Wang, H.M., Chen, X., Zhu, Z.M., Gu, Y.C., Qin, Y.M., Liu, J.L., Wang, Y.C., 2017. Overview on Critical Zone Observatory at Dajiuhu Peatland, Shennongjia. Earth Science 42(6), 1026–1038. https://doi.org/10.3799/dqkx.2017.081

Huang, X.Y., Pancost, R.D., Xue, J.T., Gu, Y.C., Evershed, R.P., Xie, S.C., 2018. Response of carbon cycle to drier conditions in the mid-Holocene in central China. Nat. Commun. 9, 1369. https://doi.org/10.1038/s41467-018-03804-w

IPCC, 2021. Climate Change 2021: the Physical Science Basis. Contribution of Working Group I to the Sixth Assessment Report of the Intergovernmental Panel on Climate Change. Cambridge University Press, New York.

Klein, E.S., Booth, R.K., Yu, Z.C., Mark, B.G., Stansell, N.D., 2013. Hydrology-mediated differential response of carbon accumulation to late Holocene climate change at two peatlands in Southcentral Alaska. Quat. Sci. Rev. 64, 61–75. https://doi.org/10.1016/j.quascirev.2012.12.013

Le, X.Q., Wu, H.B., Zhang, W.C., Li, Q., Yu, J., Liu, H., Yu, Y.Y., 2021. Peatland initiation in China associated with climate changes since the Lat Glacial Maximum. Quat. Sci. 41, 1021–1030. https://doi.org/10.11928/j.issn.1001-7410.2021.04.12

Li, H.C., Liew, P.M., Seki, O., Kuo, T.S., Kawamura, K., Wang, L.C., Lee, T.Q., 2013. Paleoclimate variability in central Taiwan during the past 30 Kyrs reflected by pollen, $\delta^{13}C_{TOC}$, and n-alkane-δD records in a peat sequence from Toushe Basin. J. Asian Earth Sci. 69, 166–176. https://doi.org/10.1016/j.jseaes.2012.12.005

Limpens, J., Berendse, F., Blodau, C., Canadell, J.D., Freeman, C., Holden, J., Roulet, N., Rydin, H., Schaepman-Strub, G., 2008. Peatlands and the carbon cycle: from local processes to global implications – a synthesis. Biogeosciences 5, 1475–1491.

https://doi.org/10.5194/bg-5-1475-2008

Lin, J., Jiang, W.Y., Wang, L., Zhang, E.L., Tang, L.Y., Yang, X.X., Chu, G.Q., Yang, S.L., Xiao, J.L., 2022. Spatially diverse hydroclimatic response to the 4.2 ka event in the Asian monsoon region. Quat. Sci. Rev. 296, 107809. https://doi.org/10.1016/j.quascirev.2022.107809

Liu, B., Zhao, H., Li, S.H., Jin, H.L., Li, Y., Wang, H.P., Sun, A.J., Xu, Y.J., Wang, K.Q., 2022. Asynchronous palaeosol development during the past 20 ka in response to climate change across the dune fields of the Asian summer monsoonal boundary, northern China. Earth Sci. Rev. 234, 104232. https://doi.org/10.1016/j.earscirev.2022.104232

Liu, G., Li, X., Chiang, H.-W., Cheng, H., Yuan, S., Chawchai, S., He, S., Lu, Y., Aung, L.T., Maung, P.M., Tun, W.N., Oo, K.M., Wang, X., 2020. On the glacial-interglacial variability of the Asian monsoon in speleothem $\delta^{18}O$ records. Sci. Adv. 6, eaay8189. https://doi.org/10.1126/sciadv.aay8189

Liu, H.Y., Gu, Y.S., Yu, Z.C., Huang, C.J., Ge, J.W., Huang, X.Y., Xie, S.C., Zheng, M., Zhang, Z.Q., Cheng, S.G., 2020. Holocence peatland water regulation response to ~1000-year solar cycle indicated by phytoliths in central China. J. Hydrol. 589, 125169. https://doi.org/10.1016/j.jhydrol.2020.125169

Liu, H.Y., Gu, Y.S., Ge, J.W., Yu, Z.C., Xu, X.N., Zhang, Z.Q., Cheng, S.G., Xie, S.C., 2022. The response of the Dajiuhu Peatland ecosystem to hydrological variations: Implications for carbon sequestration and peatlands conservation. J. Hydrol. 612, 128307. https://doi.org/10.1016/j.jhydrol.2022.128307

Liu, L.J., Chen, H., Yu, Z.C., Zhu, D., He, Y.X., Liu, J.L., Zhu, Q.A., Liu, X.W., Liu, L.F., 2020. Peatland development and carbon dynamics since the Last Glacial Maximum in the

Hengduan Mountains Region. Catena 190, 104525. https://doi.org/10.1016/j.catena.2020.104525

Ma, C.M., Zhu, C., Zheng, C.G., Yin, Q., Zhao, Z.P., 2009. Climate changes in East China since the Late-glacial inferred from high-resolution mountain peat humification records. Sci. China Ser. D-Earth Sci. 52, 118–131. https://doi.org/10.1007/s11430-009-0003-5

MacDonald, G.M., Beilman, D.W., Kremenetski, K.V., Sheng, Y.W., Smith, L.C., Velichko, A.A., 2006. Rapid Early Development of Circumarctic Peatlands and Atmospheric CH_4 and CO_2 Variations. Science 314, 285–288. https://doi.org/10.1126/science.1131722

Mampuku, M., Yamanaka, T., Uchida, M., Fujii, R., Maki, T., Sakai, H., 2008. Changes in C3/C4 vegetation in the continental interior of the Central Himalayas associated with monsoonal paleoclimatic changes during the last 600 kyr. Clim. Past 4, 1–9. https://doi.org/10.5194/cp-4-1-2008

Moore, P.D., Webb, J.A., Collinson, M.E., 1991. Pollen Analysis, second ed. Blackwell Scientific Publications, Oxford

Müller, J., Joos, F., 2020. Global peatland area and carbon dynamics from the Last Glacial Maximum to the present – a process-based model investigation. Biogeosciences 17, 5285–5308. https://doi.org/10.5194/bg-17-5285-2020

Peng, H.J., Bao, K.S., Yuan, L.G., Uchida, M., Cai, C., Zhu, Y.X., Hong, B., Guo, Q., Ding, H.W., Yao, H., Hong, Y.T., 2021. Abrupt climate variability since the last deglaciation based on a high-resolution peat dust deposition record from southwest China. Quat. Sci. Rev. 252, 106749. https://doi.org/10.1016/j.quascirev.2020.106749

Reimer, P.J., Austin, W.E.N., Bard, E., Bayliss, A., Blackwell, P.G., Ramsey, C.B., Butzin, M., Cheng, H., Edwards, R.L., Friedrich, M., Grootes, P.M., Guilderson, T.P., Hajdas, I., Heaton,

T.J., Hogg, A.G., Hughen, K.A., Kromer, B., Manning, S.W., Muscheler, R., Palmer, J.G., Pearson, C., Plicht, J. van der, Reimer, R.W., Richards, D.A., Scott, E.M., Southon, J.R., Turney, C.S.M., Wacker, L., Adolphi, F., Büntgen, U., Capano, M., Fahrni, S.M., Fogtmann-Schulz, A., Friedrich, R., Köhler, P., Kudsk, S., Miyake, F., Olsen, J., Reinig, F., Sakamoto, M., Sookdeo, A., Talamo, S., 2020. The IntCal20 northern hemisphere radiocarbon age calibration curve (0–55 cal kBP). Radiocarbon 62, 725–757. https://doi.org/10.1017/RDC.2020.41

Ribeiro, K., Pacheco, F.S., Ferreira, J.W., de Sousa-Neto, E.R., Hastie, A., Filho, G.C.K., Alvalá, P.C., Forti, M.C., Ometto, J.P., 2021. Tropical peatlands and their contribution to the global carbon cycle and climate change. Glob Change Biol. 27, 489–505. https://doi.org/10.1111/gcb.15408

Shakun, J.D., Carlson, A.E., 2010. A global perspective on Last Glacial Maximum to Holocene climate change. Quat. Sci. Rev. 29, 1801–1816. https://doi.org/10.1016/j.quascirev.2010.03.016

Tian, L.P., Wang, M.Y., Zhang, X., Yang, X.Q., Zong, Y.Q., Jia, G.D., Zheng, Z., Man, M.L., 2019. Synchronous change of temperature and moisture over the past 50 ka in subtropical southwest China as indicated by biomarker records in a crater lake. Quat. Sci. Rev. 212, 121–134. https://doi.org/10.1016/j.quascirev.2019.04.003

Treat, C.C., Kleinen, T., Broothaerts, N., Dalton, A.S., Dommain, R., Douglas, T.A., Drexler, J.D., Finkelstein, S.A., Grosse, G., Hope, G., Hutchings, J., Jones, M.C., Kuhry, P., Lacourse, T., Lähteenoja, O., Loisel, J., Notebaert, B., Payne, R.J., Peteet, D.M., Sannel, A.B.K., Stelling, J.M., Strauss, J., Swindles, G.T., Talbot, J., Tarnocai, C., Verstraeten, G., Williams, C.J., Xia,

Z.Y., Yu, Z.C., Väliranta, M., Hättestrand, M., Alexanderson, H., Brovkin, V., 2019. Widespread global peatland establishment and persistence over the last 130,000 y. Proc. Nat. Acad. Sci. 116, 4822–4827. https://doi.org/10.1073/pnas.1813305116

van Bellen, S., Dallaire, P.L., Garneau, M., Bergeron, Y., 2011. Quantifying spatial and temporal Holocene carbon accumulation in ombrotrophic peatlands of the Eastmain region, Quebec, Canada. Global Change Biol. 25, GB2016. https://doi.org/10.1029/2010GB003877

Wang, B., Ho, L., 2002. Rainy Season of the Asian–Pacific Summer Monsoon. J. Clim. 15, 386–398. https://doi.org/10.1175/1520-0442(2002)015<0386:RSOTAP>2.0.CO;2

Wang, M., Chen, H., Wu, N., Peng, C.H., Zhu, Q.A., Zhu, D., Yang, G., Wu, J.H., He, Y.X., Gao, Y.H., Tian, J.Q., Zhao, X.Q., 2014. Carbon dynamics of peatlands in China during the Holocene. Quat. Sci. Rev. 99, 34–41. https://doi.org/10.1016/j.quascirev.2014.06.004

Wang, M.Y., Zheng, Z., Man, M.L., Hu, J.F., Gao, Q.Z., 2017. Branched GDGT-based paleotemperature reconstruction of the last 30,000 years in humid monsoon region of Southeast China. Chem. Geol. 463, 94–102. https://doi.org/10.1016/j.chemgeo.2017.05.014

Wang, Y.J., Cheng, H., Edwards, R.L., He, Y.Q., Kong, X.G., An, Z.S., Wu, J.Y., Kelly, M.J., Dykoski, C.A., Li, X.D., 2005. The Holocene Asian monsoon: Links to solar changes and North Atlantic climate. Science 308, 854–857. https://doi.org/10.1126/science.1106296

Wei, Z.Q., Zhong, W., Shang, S.T., Xue, J.B., Ouyang, J., Zhu, C., Tian, L.X., Chen, Y., Chen, B., 2018. Carbon accumulation in Dahu Swamp in the eastern Nanling Mountains (South China) and its implications for hydroclimatic variability over the past 47 000 years. Boreas 47, 469–480. https://doi.org/10.1111/bor.12279

Wu, Z.Y., 1980. Vegetation of China. Science Press, Beijing.

Xu, H., Liu, B., Lan, J.H., Sheng, E.G., Che, S., Xu, S., 2013. Holocene peatland development

along the eastern margin of the Tibetan Plateau. Quat. Res. 80, 47–54. https://doi.org/10.1016/j.yqres.2013.04.001

Xu, H., Lan, J.H., Sheng, E.G., Liu, Y., Liu, B., Yu, K.K., Ye, Y.D., Cheng, P., Qiang, X.K., Lu, F.Y., Wang, X.L., 2016. Tropical/subtropical peatland development and global CH_4 during the Last Glaciation. Sci. Rep. 6, 30431. https://doi.org/10.1038/srep30431

Yu, X.F., Chen, J.Q., Zheng, Y.H., Zhong, W., Ouyang, Z.T., Zhou, W.J., 2020. Anti-phase variation of hydrology and in-phase carbon accumulations in two wetlands in southern and northern China since the Last Deglaciation. Front. Earth Sci. 8, 192. https://doi.org/10.3389/feart.2020.00192

Yu, Z.C., Loisel, J., Brosseau, D.P., Beilman, D.W., Hunt, S.J., 2010. Global peatland dynamics since the Last Glacial Maximum. Geophys. Res. Lett. 37, L13402. https://doi.org/10.1029/2010GL043584

Yue, Y.F., Zheng, Z., Huang, K.Y., Chevalier, M., Chase, B.M., Carré, M., Ledru, M.P., Cheddadi, R., 2012. A continuous record of vegetation and climate change over the past 50,000 years in the Fujian Province of eastern subtropical China. Palaeogeogr. Palaeoclimatol. Palaeoecol. 365–366, 115–123. https://doi.org/10.1016/j.palaeo.2012.09.018

Zhang, M.M., Bu, Z.J., Jiang, M., Wang, S.Z., Liu, S.S., Jin, Q., Shi, P.H., 2019. Mid-late Holocene maar lake-mire transition in northeast China triggered by hydroclimatic variability. Quat. Sci. Rev. 220, 215–229. https://doi.org/10.1016/j.quascirev.2019.07.027

Zhang, M.M., Huang, X.Y., Chen, X., 2021. Distribution Patterns and Controlling Factors of Peatlands in Subtropical Mountainous Areas of China. Wetland Science 19, 753–761. https://doi.org/10.13248/j.cnki.wetlandsci.2021.06.011

Zhang, M.M., Smol, J.P., Bu, Z.J., 2023. Holocene initiation and expansion of the southern

margins of northern peatlands triggered by the East Asian summer monsoon recession. Geosci. Front. 14, 101526. https://doi.org/10.1016/j.gsf.2022.101526

Zhang, W.C., Yan, H., Cheng, P., Lu, F.Y., Li, M., Dodson, J., Zhou, W.J., An, Z.S., 2016. Peatland development and climate changes in the Dajiuhu basin, central China, over the last 14,100 years. Quat. Int. 425, 273–281. https://doi.org/10.1016/j.quaint.2016.06.039

Zhang, W.C., Yan, H., Dodson, J., Cheng, P., Liu, C.C., Li, J.Y., Lu, F.Y., Zhou, W.J., An, Z.S., 2018. The 9.2 ka event in Asian summer monsoon area: the strongest millennial scale collapse of the monsoon during the Holocene. Clim. Dyn. 50, 2767–2782. https://doi.org/10.1007/s00382-017-3770-2

Zhang, X., Zheng, Z., Huang, K.Y., Yang, X.Q., Tian, L.P., 2020. Sensitivity of altitudinal vegetation in southwest China to changes in the Indian summer monsoon during the past 68000 years. Quat. Sci. Rev. 239, 106359. https://doi.org/10.1016/j.quascirev.2020.106359

Zhang, X., Zheng, Z., Huang, K.Y., Cheng, J., Cheddadi, R., Zhao, Y., Liang, C., Yang, X.Q., Wan, Q.C., Tang, Y.J., Chen, C., Li, J., 2023. Quantification of Asian monsoon variability from 68 ka BP through pollen-based climate reconstruction. Sci. Bull. 68, 713–722. https://doi.org/10.1016/j.scib.2023.03.013

Zhang, Z.Q., Xing, W., Wang, G.P., Tong, S.Z., Lv, X.G., Sun, J.M., 2015. The peatlands developing history in the Sanjiang Plain, NE China, and its response to East Asian monsoon variation. Sci. Rep. 5, 113116. https://doi.org/10.1007/10.1038/srep11316

Zhao, Y., Yu, Z.C., Tang, Y., Li, H., Yang, B., Li, F.R., Zhao, W.W., Sun, J.H., Chen, J.H., Li, Q., Zhou, A.F., 2014. Peatland initiation and carbon accumulation in China over the last 50,000 years. Earth Sci. Rev. 128, 139–146. https://doi.org/10.1016/j.earscirev.2013.11.003

Zheng, Z., Wei, J.H., Huang, K. Y., Xu, Q.H., Lu, H.Y., Tarasov, P., Luo, C.X., Beaudouin, C.,

Deng, Y., Pan, A.D., Zheng, Y.W., Luo, Y. L., Nakagawa, T., Li, C.H., Yang, S.X., Peng, H.H., Cheddadi, R., 2014. East Asian pollen database: Modern pollen distribution and its quantitative relationship with vegetation and climate. J. Biogeogr. 41, 1819–1832. https://doi.org/10.1111/jbi.12361

Zheng, Z., Chen, C., Huang, K.Y., Zhang, X., Kershaw, P., Cheng, J., Li, J., Yue, Y.F., Wan, Q.C., Zhang, Y.Z., Tang, Y.J., Wang, M.Y., Xiao, X.Y., Cheddadi, R., 2023. Holocene warming and evergreen/deciduous forest replacementacross eastern China. Quat. Sci. Rev. 307, 108057. https://doi.org/10.1016/j.quascirev.2023.108057

Zhou, W.J., Yu, X.F., Jull, A.J.T., Burr, G., Xiao, J.Y., Lu, X.F., Xian, F., 2004. High-resolution evidence from southern China of an early Holocene optimum and a mid-Holocene dry event during the past 18,000 years. Quat. Res. 62, 39–48. https://doi.org/10.1016/j.yqres.2004.05.004

Zhong, W., Xue, J.B., Cao, J.X., Zheng, Y.M., Ma, Q.H., Ouyang, J., Cai, Y., Zeng, Z.G., Liu, W., 2010. Bulk organic carbon isotopic record of lacustrine sediments in Dahu Swamp, eastern Nanling Mountains in South China: Implication for catchment environmental and climatic changes in the last 16,000 years. J. Asian Earth Sci. 38, 162–169. https://doi.org/10.1016/j.jseaes.2009.12.011